A Tool to Estimate the Phase Velocity Dispersion of Different Lamb Wave Modes Using Datasets of Two Signals Measured at Identical Distances

Lina Draudvilienė and Asta Meškuotienė

***Abstract*—This study introduces an approach for evaluating the phase velocity dispersion of the Lamb wave both A_0 and S_0 modes using only two signals measured at identical distances. To select two suitable measurement points, it is first necessary to calculate the maximum possible distance between the two signals. Once a packet of two signals has been received to select the appropriate threshold level. Theoretical and experimental investigations are conducted using A_0 and S_0 mode signals at a 300-kHz frequency range propagating through an aluminum plate. Four pairs of signals for each A_0 and S_0 mode measured at the same distances are employed in the theoretical analysis. The calculated mean relative error consistently remained below 0.5% in all cases. Similarly, six pairs of signals are used in the experimental study, and the relative error on average remained below 2%. A comprehensive uncertainty analysis is conducted to assess the method's reliability. The study explored the impact of various error sources on velocity measurement parameters and discussed their significance for both A_0 and S_0 modes. The mean relative error of 1.7% for the A_0 and of 2% for the S_0 modes are obtained, along with extended uncertainties of $\pm$2.6% and $\pm$3.2% at a 95% confidence level, respectively. The proposed tool is suitable for determining two suitable measurement points and estimating the phase velocity of both A_0 and S_0 modes of Lamb waves. This approach offers an advantage by eliminating the need for time-consuming object scanning.**

***Index Terms*—Accuracy, asymmetric mode, dispersion curves, frequency, Lamb waves, phase velocity, symmetric mode, uncertainty, zero-crossing method.**

I. Introduction

LAMB waves are effective in detecting cracks, corrosion, delamination, material fatigue, and so on in various types of structures and are therefore widely used in a wide range of industrial applications [1], [2]. These waves can propagate inside the thin wall structure over significant distances with low attenuation and high sensitivity to structural changes [3], [4]. Therefore, these waves have been successfully used for structural health monitoring (SHM) and nondestructive testing (NDT) applications. However, the two main inherent properties of Lamb waves, such as dispersion, which is manifested by velocity variations with frequency and characterized by phase and group velocities and an infinite number of modes, make their application difficult [3], [5]. Therefore, the different signal processing methods (SPMs) have to be used for the evaluation of the group and phase velocities. Since this work concerns phase velocity and the analysis of a specific SPM for its determination, the difficulties and limitations affecting phase velocity determination are discussed in the following.

One characteristic of Lamb wave signals propagating through a dispersive medium is that different frequency components propagate at different velocities, which leads to distortion of the overall waveform [6]. Depending on the propagation distance, the signal amplitude decreases and the waveform elongates [7]. This phenomenon makes it difficult to identify the same phase point in the signal waveform. Therefore, the objects are scanned at multiple locations along the wave propagation path, and the specific SPMs are used to estimate the phase velocity. Numerous (SPMs) have been developed and applied. These techniques include the 2-D fast Fourier transform (2D-FFT) and its variations, the wavelet transform (WT), the Wigner–Ville distribution (WVD), and its variations, and among others [8], [9]. However, using these methods, the time required for scanning limits rapid data acquisition, as the process is time-consuming and labor-intensive. Thus, new approaches are being explored to expand the use of Lamb waves and obtain the most comprehensive and reliable information possible without scanning. One such approach is to estimate phase velocity using only two signals. The SPMs for evaluating the phase velocity of dispersive modes using only two signals are currently under development and being studied for their applicability. The SPMs, such as the short-time chirp-Fourier transform (STCFT) method [10] and a combined Hilbert transform and cross correlation technique [11], have been proposed. These methods reconstruct the segments of the phase velocity dispersion curves using two received signals. However, some key limitations to the application of these methods should be given.

A special chirp signal is used to generate the Lamb waves when applying the STCFT method [10]. This method of generation makes it difficult to identify the A_0 and S_0 modes separately depending on the distance. The choice of the

Received 12 March 2025; revised 29 May 2025; accepted 1 June 2025. Date of publication 16 June 2025; date of current version 14 July 2025. This work was supported by the Research Council of Lithuania through the Project COMMET—A Combined Signal Processing Method for Determining the Location and Size of Defects Using Higher-Order Ultrasound Guided Waves under Grant MIP-23-119. The Associate Editor coordinating the review process was Dr. Dong Wang. *(Corresponding author: Lina Draudvilienė.)*

Lina Draudvilienė is with the Ultrasound Research Institute, Kaunas University of Technology, 51423 Kaunas, Lithuania (e-mail: lina.draudviliene@ktu.lt).

Asta Meškuotienė is with the Institute of Metrology, Kaunas University of Technology, 51368 Kaunas, Lithuania (e-mail: asta.meskuotiene@ktu.lt).

Digital Object Identifier 10.1109/TIM.2025.3579845

distance between two adjacent signals is not given, and there is no analysis of what parameters have to be estimated, what signal characteristics influence the choice of the two measurement points, and the resulting experimental errors are up to 10% in certain frequency ranges. The next method is a combined Hilbert transform and cross correlation method proposed to estimate the phase velocity of the A_0 and S_0 modes [11]. This method is very sensitive to mode shape distortion, and the measurement points for the A_0 and S_0 modes were chosen at different wave propagation distances. There are any justification as to how the distance between the two measurement points was chosen, nor did it analyze what parameters or wave propagation characteristics affect this choice, and the analysis of the errors was not given. It is then difficult to determine and assess the reliability with which the method works. Our previous study [12] has shown that the phase velocity dispersion curves of the A_0 and S_0 modes can be reconstructed using two signals obtained for each mode in a combined zero-crossing and spectral decomposition approach. It was found that using this method, the distance between two measurement points for the S_0 mode must be greater than that for the A_0 mode; otherwise, large errors are obtained. Other authors have used a clustering algorithm to calculate the phase velocity [13], stating that the number of points is a crucial element in its calculation using this algorithm. Thus, the segments of the phase velocity dispersion curves for the A_0 and S_0 modes were obtained using ten measurement points. Therefore, reliable methods are sought to estimate the phase velocity of different Lamb wave modes using as few measurement points as possible, while avoiding scanning.

Our previous work [6] explored how to evaluate the phase velocity of the dispersive A_0 mode using the signals measured only at two positions. It was found that in order to obtain suitable signals to estimate the phase velocity dispersion, the maximum possible distance between the two measurement points must be known. This parameter thus limits the measurement basis, which makes the selection of the appropriate two measurement points difficult. The study has presented how to determine the maximum possible distance between two measurement points, and on this basis, the phase velocity dispersion curves of the A_0 mode at different frequency ranges have been reconstructed using the zero-crossing method. The results obtained demonstrated the feasibility of the zero-crossing method for the estimation of the phase velocity of the A_0 mode using only two signals, since the calculated mean relative error was no more than 1.4% in the experimental study [6].

Other authors have used a clustering algorithm to calculate the phase velocity [13] and state that the number of points is a crucial element in the calculation of the phase velocity using this algorithm. Thus, the average relative error of the measured Lamb A_0 or S_0 dispersion curves propagating in the aluminum plate was obtained within 1% but using ten measurement points. Our previous study [12] has shown that the phase velocity dispersion curves of the A_0 and S_0 modes can be reconstructed using two signals in a combined zero-crossing and spectral decomposition approach. The experiment shows that the A_0 mode is reproduced with 1.04% and the S_0 mode with 0.6%. However, it should be pointed out that such higher accuracies have been obtained using signal pairs measured at different distances for both modes.

The next step of the study is to present how time and effort can be further minimized while more information can be obtained. The signals of the asymmetric A_0 and symmetric S_0 modes carry different information as they propagate through the medium. This means that it is important to develop a method that can obtain information from both modes quickly and reliably.

This study aims to present a method for reconstructing the phase velocity dispersion curves of the A_0 and S_0 Lamb wave modes using datasets of two signals measured at identical distances; identify the main parameters and principles to be evaluated in order to select suitable pairs of two signals for different modes; and assess the method's reliability through a comprehensive error and uncertainty analysis, including characteristic quantification.

The research is divided into three main sections: a theoretical study, an experimental study, and an evaluation of the method's reliability characteristics. Section II delves into the fundamental principles and computational methods for analyzing Lamb wave propagation. Section III focuses on the practical implementation and validation of the proposed method. Section IV dedicated to assess the method's robustness and limitations. It identifies and quantifies potential sources of uncertainty, providing a comprehensive analysis of accuracy to establish the method's overall reliability and its comparability with the existing techniques.

II. Theoretical Study

A. Simulation of Signals

The aluminum plate with a thickness of 2 mm was used in the study. The plate had the following elastic properties: density $\rho = 2710$ kg/m^3, Young modulus $E = 71.7$ GPa, and Poisson's ratio $\nu = 0.33$. A three-period, 300-kHz harmonic burst with a Gaussian envelope was used as the incident signal, $u_0(t)$. The set of simulated A_0 mode signals was obtained by applying the simplified complex transfer function of Lamb waves propagating in the selected medium [14]

$$u(x,t) = \frac{1}{2\pi}\int_{-\infty}^{\infty} \mathrm{FT}\left(u_0(t)\right) e^{-j\omega\frac{x}{c_p(\omega)}} e^{j\omega t} d\omega \tag{1}$$

where $u_0(t)$ is the excitation signal, FT is the Fourier transform, t is the time, $\omega = 2\pi f$ is the angular frequency, f is the frequency, and j is the basic imaginary unit $j = \sqrt{-1}$. Since the attenuation of Lamb waves propagating in metal plates is very low, this parameter is neglected [15].

The received signals $u(x, t)$ for both A_0 and S_0 modes of Lamb waves were calculated at 0–200 mm with a step of 0.1 mm and 2001 simulated signals are obtained. The B-scan images of both modes are presented in Fig. 1(a) and (b), respectively.

The B-scans of both A_0 and S_0 modes Fig. 1(a) and (b) clearly indicate the differences in the phase velocity propagation between these modes at 300-kHz frequency range [6].

The A_0 mode exhibits significant dispersion, with distinct phase and group velocities $c_{\mathrm{ph}} = 1999$ m/s and $c_{\mathrm{gr}} = 2972$ m/s,

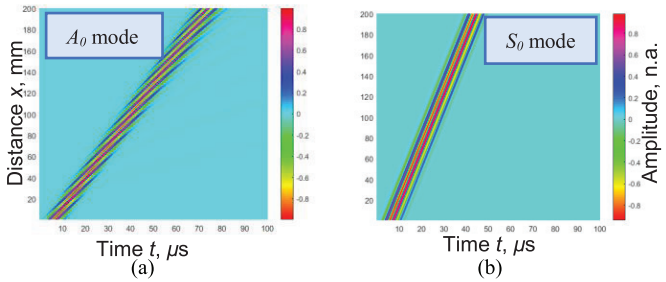

Fig. 1. B-scan image of the simulated (a) A_0 mode and (b) S_0 mode.

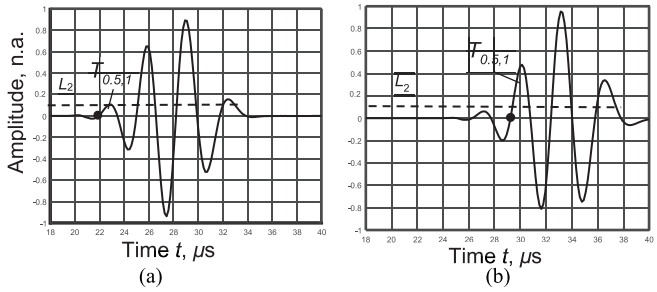

Fig. 2. A mode signals measured at distances (a) x_1 = 63 mm and (b) x_4 = 81 mm.

respectively, while the S_0 mode is either not dispersive or only slightly dispersive c_{ph} = 5380 m/s and c_{gr} = 5314 m/s.

It has been shown [14] that the maximum distance Δl between two suitable signals can be determined from the phase and group velocity dispersion curves calculated analytically (e.g., using the SAFE method). The maximum distance Δl is calculated according to [14]

$$\Delta l \leq \frac{1}{f} \cdot \frac{c_{\text{gr}}(f) \cdot c_{\text{ph}}(f)}{\left|c_{\text{gr}}(f) - c_{\text{ph}}(f)\right|} \tag{2}$$

where $c_{\text{gr}}(f)$ is the group velocity at the central frequency, $c_{\text{ph}}(f)$ is the phase velocity at the central frequency, and f is the central frequency.

The conducted study clearly demonstrated that the segments of the A_0 mode phase velocity dispersion curve at various dispersion levels can be reproduced, given a corresponding pair of signals [14]. However, the specialized SPMs are required to evaluate the phase velocity of dispersive Lamb wave modes. The zero-crossing method, adapted for this purpose, is described in Section II-B.

B. Zero-Crossing Method

The zero-crossing algorithm divides a signal into half-periods based on identified zero-crossing points. This algorithm consists of four main steps: selecting a threshold level L; calculating phase velocity values ($c_{\text{ph}n}$); determining frequency values (f_n); and pairing these values $\{f_n, c_{\text{ph}n}\}$ [6].

1) *Threshold Level Selection L:* As a prerequisite, the time points crossing the zero-amplitude line must be chosen, so that the same phase point is detected for both selected signals. The threshold level is thus a critical parameter for the correct determination of the time instants. Therefore, how to select this parameter will be discussed in the next section using the datasets of two signals of the dispersive A_0 mode.
2) *Calculation of the Phase Velocity Values (c_{ph}):* Time instants at which both signals cross the zero-amplitude line $t_1(x_1), t_2(x_1), \ldots, t_N(x_1)$ and $t_1(x_2), t_2(x_2), \ldots, t_N(x_2)$ are measured. The phase velocity values are calculated using expression

$$c_{\text{ph},k} = \frac{x_2 - x_1}{t_k(x_2) - t_k(x_1)} \tag{3}$$

where $k = 1, 2, \ldots, N$; k is the number of zero-crossing instant in the signals; N is the total number of measured zero-crossing instants in the signals. In this way, the time of flight (ToF) values of both signals are fixed according to the zero-crossing points, and then, the phase velocity values are calculated.
3) The equivalent frequencies corresponding to the calculated duration of each selected half-period of second signal are estimated. The duration of second signal selected half-periods $T_{0.5,1}(x_2), T_{0.5,2}(x_2), \ldots, T_{0.5,N-1}(x_2)$ are calculated by

$$T_{0.5,k}(x_2) = t_{k+1}(x_2) - t_k(x_2). \tag{4}$$

Determination of the frequency value ($f_{0.5,k}$) for the dispersion curve reconstruction

$$f_{0.5,k} = \frac{1}{2T_{0.5,k(x_2)}}. \tag{5}$$

4) The phase velocity dispersion curve segment is determined, which is described by creating sets of pairs of frequencies $f_{0.5,k}$ and determined phase $c_{\text{ph},k}$ velocities

$$\left\{f_{0.5,k}, c_{\text{ph},k}\right\}. \tag{6}$$

Thus, the zero-crossing algorithm requires only two signals per mode to determine phase velocity values and only one signal per mode to determine frequency values. By pairing the calculated phase velocity and frequency values, a segment of the phase velocity dispersion curve is reconstructed. How to apply this method and to determine necessary parameters is presented in Section II-C.

C. Phase Velocity Evaluation of the A_0 Mode

The maximum distance Δl between two suitable signals should be known. According to (1), this distance is calculated and, in this case, is Δl = 19 mm. Four signals at different distances are selected for the study: x_1 = 63 mm, x_2 = 68 mm, x_3 = 73 mm, and x_4 = 81 mm (Fig. 2). Three pairs of the signals are used for the study. The selected different distances between the two signals are used to explain what difficulties are encountered and how to resolve them. The two signals at distances x_1 = 63 mm and x_4 = 81 mm are presented in Fig. 2(a) and (b), respectively.

The question is whether the zero-crossing points can be properly selected from the obtained waveforms. According to the algorithm presented in Section II-B, in order to determine the correct zero-crossing points for both analyzing signals,

TABLE I
SELECTION OF THRESHOLD LEVEL L FOR THE A_0 MODE

Selected pairs of two signals ($x_1 - x_2$), mm	Distance between signals Δl, mm	Threshold L	Mean relative error $\bar{\delta}_{c_{ph}}$, %
(63 – 68)	5	0.2	0.14
(63 – 73)	10		64
(63 – 81)	18		35
(63 – 68)	5	0.1	0.6
(63 – 73)	10		0.4
(63 – 81)	18		0.1
(63 – 68)	5	0.08	0.6
(63 – 73)	10		0.4
(63 – 81)	18		33

first, the appropriate threshold level L should be selected. Thus, three different threshold levels: $L_1 = 0.2$, $L_2 = 0.1$, and $L_3 = 0.08$ are selected for the study. The mean relative error is calculated in each case according to

$$\bar{\delta}_{c_{\text{ph}}} = 100\% \cdot \frac{1}{N} \sum_{n=1}^{N} \frac{\left| c_{\text{ph}} - c_{\text{ph}}^{\text{SAFE}} \right|}{c_{\text{ph}}^{\text{SAFE}}} \tag{7}$$

where c_{ph} is the value of the phase velocity calculated by the zero-crossing algorithm and $c_{\text{ph}}^{\text{SAFE}}$ are the values of the phase velocity calculated by the analytical method.

Thus, using $L_1 = 0.2$, $\bar{\delta}_{c_{\text{ph}}} = 35\%$ is obtained. As mentioned above, the dispersion influences the change in waveform depending on the propagation distance. Thus, the first zero crossing point is determined at different half-periods of both signals using the threshold level of $L_1 = 0.2$. In this way, the ToF is measured between phase points that are in different half-periods, which means that these phase poins are not the same. The obtained $\bar{\delta}_{c_{\text{ph}}} = 0.1\%$ clearly indicates that $L_2 = 0.1$ is suitable for further calculations. The first zero-crossing point for both signals is determined in the same half-periods [Fig. 2(a) and (b)]. $\bar{\delta}_{c_{\text{ph}}} = 33\%$ is obtained using the threshold level of $L_3 = 0.08$. The same situation is obtained as in case with $L_1 = 0.2$, and the first zero crossing point is determined at different half-periods of both signals. Thus, it is not possible to immediately determine visually which threshold level is appropriate from the waveforms. Each selected threshold level was applied to all selected pairs of signals, and the mean relative error was calculated in each case. The obtained results are presented in Table I.

The calculated mean relative errors in each analyzed case clearly show which threshold levels are suitable for phase velocity estimation. The selected distance at $x_1 = 63$ mm and $x_2 = 68$ mm, and selecting $L_1 = 0.2$, an average relative error of 64% is obtained. Meanwhile, a mean relative error of 0.6% is obtained if the selected threshold levels are $L_2 = 0.1$ and 0.08 for the same analyzed signals. The selected threshold level of $L_2 = 0.1$ is suitable for all sets of two signals (Table I). The selected level of $L_3 = 0.08$ is not suitable using signals at distances $x_1 = 63$ mm and $x_2 = 81$ mm. It should be noted that the smaller the measurement distance between the two signals, the higher error obtained. When the distance between the two signals is 18 mm, the mean relative error is only 0.1%. Meanwhile, if this distance is 5 mm, it is 0.6%. Thus, to select an appropriate threshold level, a simple algorithm based on an iterative fit to the analytically calculated phase velocity dispersion curve (obtained, for example, using the SAFE method) can be employed. The algorithm for determining the suitable threshold level L is illustrated in Fig. 3.

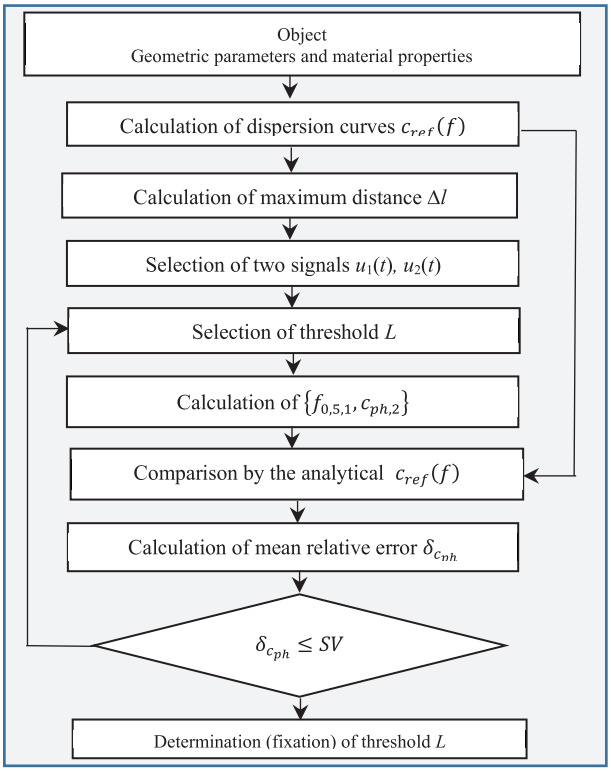

Fig. 3. Flowchart of the algorithm for determining the suitable threshold level L(SV-selected value).

TABLE II
SUITABLE DISTANCE BETWEEN TWO SIGNALS FOR THE S_0 MODE

Selected pairs of two signals ($x_1 - x_2$), mm	Distance between signals Δl, mm	Threshold L	Mean relative error $\bar{\delta}_{c_{ph}}$, %
(63 – 65)	2	0.2	0.6
(63 – 70)	7		0.4
(63 – 75)	12		0.36
(63 – 81)	18		0.08

The calculated mean relative error indicates the suitability of the selected threshold level. Therefore, it is essential to establish a maximum permissible relative error and select the threshold level accordingly. In this theoretical study, a maximum relative error limit of 1% is used. Thus, once a set of phase velocity and frequency values that meets the established criterion SV is obtained, the remaining values are calculated according to the presented algorithm.

D. Nondispersive S_0 Mode

Appropriate measurement point selection is necessary for evaluating the S_0 mode phase velocity. The set of theoretically calculated S_0 mode signals shown in Fig. 1(b) is used for this analysis. This mode is nearly nondispersive at 300 kHz, with a difference of only approximately 66 m/s between the phase and group velocities. This indicates that the ToF can

TABLE III
METROLOGICAL PARAMETERS OF RECONSTRUCTED DISPERSION CURVES USING THE SIMULATED SIGNALS

Modes	Selected pairs of two signals ($x_1 - x_2$)	Threshold, L	Mean absolute error $\overline{\Delta}_{mod}$	Mean relative error $\overline{\delta}_{mod}$	Standard deviation of the measurement model $\sigma_{\Delta_{mod}}$	Reconstructed frequency range f, kHz
A_0	(61 – 79) mm	0.08	14 m/s	0.64 %	7.3 m/s	242 – 322
S_0		0.1	7 m/s	0.13 %	6.3 m/s	295 – 307
A_0	(82 – 100) mm	0.1	18.7 m/s	0.97 %	17.5 m/s	230 – 326
S_0		0.1	6.5 m/s	0.12 %	6.3 m/s	294 – 309
A_0	(121 – 139) mm	0.11	18.5 m/s	0.95 %	11.3 m/s	238 – 333
S_0		0.1	5.1 m/s	0.12 %	4.6 m/s	291 – 312
A_0	(180 – 198) mm	0.12	18 m/s	0.9 %	11.5 m/s	249 – 340
S_0		0.1	5.5 m/s	0.1 %	5.3 m/s	288 – 16

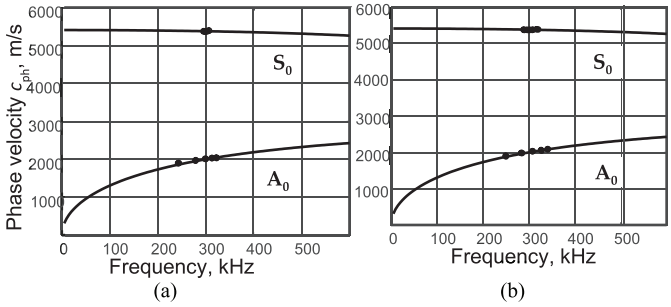

Fig. 4. Obtained segments of the phase velocities for the A_0 and S_0 modes (dots) are plotted together with those calculated by the SAFE method using signals at the distances (a) x_{61} = 61 mm and x_{79} = 79 mm and (b) x_{180} = 180 mm.

be correctly estimated using two signals at any propagation distance and any separation between them. Therefore, using the maximum distance determined for the A_0 mode, two measurement points are selected for S_0 mode. However, as presented in [11], the large errors can occur, where small propagation distances are used for the S_0 mode. Four signal pairs at different propagation distances were selected for the S_0 mode. These selected distances are presented in Table II. Using the zero-crossing algorithm with a threshold level of $L = 0.2$, six zero-crossing points were identified for each signal. The obtained results are presented in Table II.

The results clearly show that using a shorter intersignal distance leads to larger errors in the S_0 mode phase velocity calculation (Table II). The calculated average relative error is 0.6% with a 2-mm separation, compared to only 0.08% with an 18-mm separation. The same regularities were obtained for the A_0 mode. The smaller the measurement distance between the two signals, the higher the mean relative error obtained (Table I).

E. Phase Velocity Evaluation of Both A_0 and S_0 Modes

The theoretical study used four signal pairs for both the A_0 and S_0 modes and selected at various points along the Lamb wave propagation path. The maximum distance between two signals for the dispersive A_0 mode, calculated using (1), is 19 mm.

An 18-mm separation was chosen for all test cases and specified in Table III. The threshold level for the A_0 mode in each case was determined using the proposed algorithm (Fig. 3). For the S_0 mode, the threshold level was determined from the received waveforms of both signals and set to 0.1 for all test cases. Six zero-crossing points were identified in each case, yielding five measurement points on the dispersion curves. The segments of the phase velocity dispersion curves of both modes were reconstructed using only two signals per mode. The reconstructed segments of the phase velocity dispersion curves for the A_0 and S_0 modes, acquired at x_{61} = 61 mm and x_{79} = 79 mm and at x_{178} = 180 mm and x_{196} = 198 mm, are shown in Fig. 4(a) and (b), respectively. Table III presents the metrological parameters of the reconstructed dispersion curves obtained from the simulated signals.

The calculated mean relative errors for both A_0 and S_0 modes were consistently below 1% in all cases. This demonstrates the feasibility of reconstructing phase velocity dispersion curve segments for both A_0 and S_0 modes using only two signals per mode, measured at the same distance and at any propagation distance. To validate these theoretically results, experimental verification was conducted, the findings of which are detailed in Section III.

III. EXPERIMENTAL STUDY

To validate the theoretical results and assess the method's reliability, an experimental study was conducted on a homogeneous aluminum plate with dimensions of (1.1 × 0.62) m^2 and a thickness of 2 mm. The plate's material properties were consistent with those described in Section II-A. Wideband, contact-type ultrasonic transducers with a 180-kHz resonant frequency and a bandwidth from 40 to 640 kHz (−10 dB) [16] were used in the experimental study. The transmitter was excited by a three-period Gaussian envelope signal, generated and received by the "Ultralab" ultrasonic measurement system, which included a voltage generator, a low-noise amplifier, and an analog-to-digital converter. Signals were recorded at a 100-MHz sampling frequency. A transmitter on the aluminum plate's surface excited both A_0 and S_0 modes, and the receiver recorded the signals at selected distances. Six signal pairs at different propagation distances were chosen for the study. To improve the signal-to-noise ratio (SNR), seven measurements were taken and averaged for each case. Averaging is a well-established technique for SNR improvement in ultrasonic measurements, reducing the impact of uncorrelated noise [17].

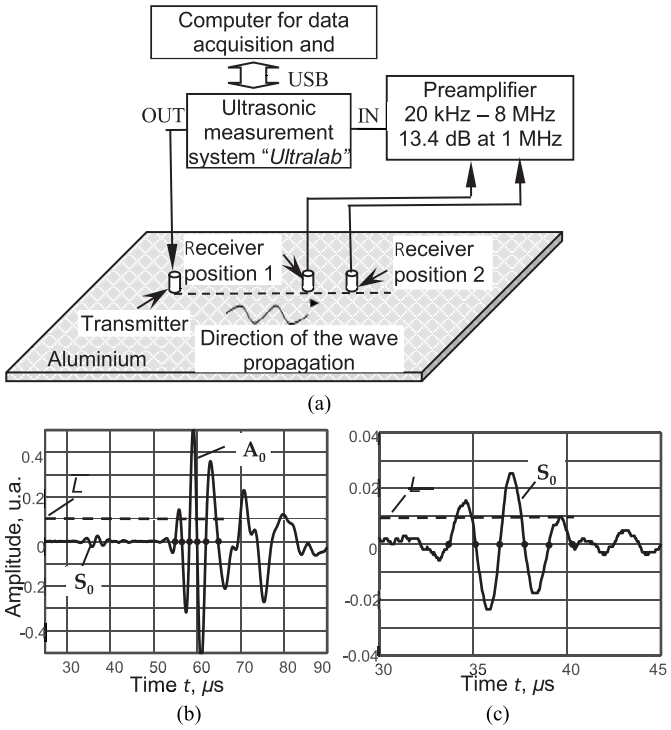

Fig. 5. (a) Experimental measurement setup, (b) waveforms of the A_0 and S_0 modes acquired at the distance of x_{168} = 168 mm from the transmitter, and (c) S_0 mode signal x_{168} = 168 mm.

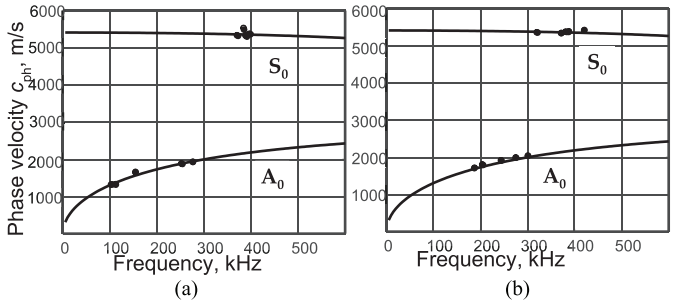

Fig. 6. Reconstructed segments of the phase velocities of the A_0 and S_0 modes (dots) are plotted together with those calculated by the SAFE method using signals at the distances (a) x_{90} = 90 mm and x_{108} = 108 mm and (b) x_{240} = 240 mm and x_{258} = 258 mm.

The ultrasonic signal remains coherent over multiple waveform acquisitions, while random noise varies unpredictably. For example, by doubling the number of averaged acquired waveforms, the SNR can be increased by approximately 3 dB.

An experimental setup for generating and receiving the Lamb wave A_0 and S_0 mode signals is presented in Fig. 5(a). The waveforms of both modes, acquired at a distance x_{168} = 168 mm from the transmitter, are presented in Fig. 5(b). In order to show more clearly the low-amplitude S_0 mode signal, this mode is shown separately in Fig. 5(c).

The threshold level was determined according to the proposed algorithm (Fig. 3) for A_0 mode. The threshold level for the S_0 mode was set to the same value of 0.01 for each investigated case. Six zero-crossing instances were determined for both A_0 and S_0 signals, and by applying the zero-crossing method, the segments of the phase velocity were reconstructed using the datasets of two signals measured at identical distances. The reconstructed segments of the phase velocities for the A_0 and S_0 modes (dots) are plotted together with those calculated by the SAFE method using signals at the distances x_{90} = 90 mm and x_{108} = 108 mm (a) and x_{240} = 240 mm and x_{258} = 258 mm (b). The obtained results are presented in Fig. 6. Table III presents the metrological parameters of reconstructed dispersion curves utilizing experimental signals.

$\Delta_{c_{\text{phmax}}}$ in the table is the maximum deviation from the average velocity error for a single point. The performed experimental study for the A_0 mode is showed that the average of $\bar{\delta}_{c_{\text{ph}}}$ across all intervals is 1.7%. As the distance between the two selected signal pairs increases, the reconstructed frequency band narrows. The minimum mean relative error of 0.7% was found at (210–228) mm, with the dispersion curve reconstructed in the frequency range of (182–298) kHz. Whereas the A_0 mode is analyzed in the range of strong dispersion, which means that the amplitude of the signal decreases with propagation distance and the waveform elongates [7], then the number of selected measurement points can be increased. For instance, instead of six, eight zero-crossing points can be considered; then, the reconstructed frequency band narrows. The minimum mean relative error of 0.7% was found at (210–228) mm, with the dispersion curve reconstructed in the frequency range of (182–298) kHz. This not only broadens the frequency range of the reconstructed curve but also increases the mean relative error by approximately 2.5 times, and it is 2.3%. Thus, the fixed seven and eight zero-crossing points introduce larger errors in the ToF determination. Meanwhile, the choice of a measurement distance of (240–258) mm distorts the waveforms even more by dispersion and results in a mean relative error of 2.55% with only six zero-crossing points. A mean relative error of 3.4% is obtained using eight zero-crossing points. Thus, the study clearly shows that in order to estimate the phase velocity of the A_0 mode as accurately as possible using a set of two measured signals, it is preferable to choose a distance close to the excitation, when the signals are not yet strongly affected by dispersion. In the present case under analysis, the appropriate distance would be up to approximately 200 mm. The S_0 mode almost is almost not dispersive in the 300-kHz range. The average of $\bar{\delta}_{c_{\text{ph}}}$ obtained across all intervals for the S_0 mode is approximately 2%. However, it should be noted that the frequency distribution is obtained in a narrow bandwidth of only 27 kHz when a close excitation distance (90–108) mm is selected. The reconstructed dispersion curve (319–420) kHz has a minimum relative error of 0.5% for the S_0 mode in the interval (240–258) mm, and the reconstructed frequency range is about 100 kHz. However, the signal amplitude decreases with distance, so a lower threshold level should be selected to determine six zero-crossing points (Table IV). In order to estimate the phase velocity of the S_0 mode in a wider frequency range, the measurement points should be selected further from the excitation zone. Thus, for the estimation of the phase velocity of both modes, it is appropriate to choose the meaurement distance approximately at (120–210) mm (Table IV). Analyzing the results obtained, it can be concluded that the phase velocity segments of the

TABLE IV
METROLOGICAL PARAMETERS OF RECONSTRUCTED DISPERSION CURVES USING THE EXPERIMENTAL SIGNALS

Modes	Selected pairs of two signals ($x_1 - x_2$), mm	Threshold L	Mean absolute error $\bar{\Delta}_{c_{ph}}$, m/s	Mean relative error $\bar{\delta}_{c_{ph}}$, %	standard deviation of the velocity (dispersion curve) $\sigma_{\Delta_{c_{ph}}}$, m/s	The maximum deviation from the mean velocity error $\Delta_{c_{phmax}}$, m/s	Frequenc y range, kHz
A_0	(90 – 108)	0.12	29.9	1.9	36.13	59.1	102 – 276
S_0		0.01	57	1.04	79.2	141	370 – 397
A_0	(120 – 138)	0.08	37.8	2.2	25.1	38.2	112 – 290
S_0		0.01	34.1	1.4	24.4	25.9	330 – 392
A_0	(150 – 168)	0.11	26.02	1.5	19.3	24.8	116 – 292
S_0		0.01	133.6	2.4	119.8	202.4	331 – 395
A_0	(190 – 208)	0.11	27.6	1.53	15.3	20.6	180 – 298
S_0		0.01	133.4	2.6	89.7	152.6	317 – 392
A_0	(210 – 228)	0.1	12.94	0.72	9.17	14.1	182 – 298
S_0		0.01	189.6	3.7	124.2	199.4	282 – 384
A_0	(240 – 258)	0.1	48.6	2.55	13.9	19.6	187 – 300
S_0		0.008	30.1	0.5	22.2	37.9	319 – 420

TABLE V
SUMMARY OF UNCERTAINTY BUDGET OF MEASUREMENT OF VELOCITY FOR A_0 AND S_0 MODES

Sources of combined standard uncertainty	Standard uncertainty σ		Distribution	Sensitivity coefficient W		Uncertainty contribution $\sigma \cdot W$	
	A_0 mode	S_0 mode		A_0 mode	S_0 mode	A_0 mode	S_0 mode
Mathematical model	11.9 m/s	5.6 m/s	Gaussian	1		12.5 m/s	5.6 m/s
Velocity (dispersion curve)	19.8 m/s	76.6 m/s	Gaussian	1		19.8 m/s	76.6 m/s
Fluctuations of the Lamb wave's frequency f	9.8 m/s	42.1 m/s	Gaussian	1		9.8 m/s	42.1 m/s
Distance between two points	$5.8 \cdot 10^{-5}$m	$5.8 \cdot 10^{-5}$m	Rectangular	$2 \cdot 10^{-5}$s	10^{-5}s	2.9 m/s	5.8 m/s
Combined standard uncertainty for mode						1.3 %	1.6 %
For A_0 mode, the mean relative error is 1.7 %, and the extended uncertainty: U= ±2.6 %, p=95 %. For S_0 mode, the mean relative error is 2 %, and the extended uncertainty: U= ±3.2 %, p=95 %.							

A_0 and S_0 modes can be reproduced using the datasets of two signals measured at identical distances.

Furthermore, a comprehensive evaluation of errors and uncertainties is performed to assess the reliability of the given tool. Evaluating the reliability of a novel method is crucial for validation, establishing confidence, identifying potential errors, facilitating comparison with the existing techniques, and ensuring overall quality [18]. Section IV details the reliability assessment performed and the results obtained.

IV. EVALUATION OF THE METHOD'S RELIABILITY CHARACTERISTICS

To determine the qualitative and quantitative estimates of Lamb wave velocity using this method, the potential sources of uncertainty were identified. The key sources can be classified into three categories: method implementation, measuring instruments, and specimen parameters [19]. The uncertainty budget for the A_0 and S_0 modes is presented in Table V.

Simulation results confirmed that errors in the dispersion curve recovery process, including noise and signal distortion, can affect the accuracy of velocity estimation. We assume that Lamb wave frequency fluctuations, which can introduce uncertainties in the measured velocities, are included in the standard deviation. The model's influence on the total uncertainty was evaluated by taking the average standard uncertainty of the model, obtained using simulated signals

$$\sigma_{\Delta_{\text{mod}}} = \sqrt{\frac{\sum_{n=1}^{N} \left(\left(\Delta_{\text{mod},n} \right) - \bar{\Delta}_{\text{mod}} \right)^2}{(N-1)}} \tag{8}$$

where N is the number of points in a segment of mathematical reconstructed dispersion curve; nth is the point of the segment; $\Delta_{\text{mod},n}$ are the errors of velocities of the reconstructed dispersion curve from the simulated signals; $\bar{\Delta}_{\text{mod}}$ is the average of errors of velocities. Analogous to (8), the standard uncertainty of reconstructing the real dispersion curve is calculated using experimental signals.

The maximum deviation from the average velocity error at any given point within the frequency range, which is considered as the uncorrected error, is detailed in Table IV. This value serves as the basis for estimating the standard uncertainty arising from fluctuations in the Lamb wave frequency f. We assume that this component allows us to assess how the operating frequency band of the transducer used in the experiment influences the constructible frequency range of the dispersion curve. By adopting a Gaussian distribution with a 99% confidence level [19], this component is calculated accordingly: $\sigma(\mathbf{\Delta}_{\boldsymbol{c}_{\text{phmax}}}) = (\mathbf{\Delta}_{\boldsymbol{c}_{\text{phmax}}}/3)$. Research indicates that the spacing between measurement points can affect the outcome of the experiment [20].

Assuming that the distance between two signals can be determined by the scanner step Δl, which is known to be 0.1 mm, the standard uncertainty can be calculated using

a rectangular distribution $\sigma(l) = \pm(\Delta l/\sqrt{3})$. The transducer emits a pulse of duration t, corresponding to the excitation of waves within a specific frequency band. The pulse onset coincides with the start of the first signal, while its termination aligns with the end of the second signal. The influence factor of $\sigma(l)$ is presented in Table V. It is calculated as the partial derivative of function f (representing the measurement outcome) with respect to the ith input parameter x_i [21] and equal to $1/t$. This uncertainty contribution fluctuates between 1.7 and 3 m/s for the A_0 mode and between 2.9 and 5.8 m/s for the S_0 mode. However, these values do not contribute to the overall uncertainty.Temperature variations, mechanical, and geometric parameters of the specimen, including density ρ, Young's modulus E, Poisson's ratio ν, and plate thickness d, can affect measurement results by altering both the geometric parameters and mechanical properties of the specimen [22], [23]. However, their impact is generally negligible for short-duration measurements conducted in controlled laboratory environments. Consequently, material properties are standardized at a reference temperature of 20 °C ± 1 °C. In this case, the results presented in Table V show that the combined uncertainty components for the A_0 mode are influenced by the mathematical model, the reconstruction of the dispersion curve, and fluctuations in the Lamb wave's frequency f. The distance estimation does not contribute to the overall uncertainty. For the S_0 mode, only two components have an impact, and the combined value of the other two components does not change the overall uncertainty, as they constitute only 0.4% of the total relative uncertainty for the S_0 mode. The combined uncertainty was calculated considering the contribution of all individual sources of uncertainty. The expanded uncertainty, which considers the confidence level, was determined using the standard formulas [21]. The extended uncertainty in Table V is presented for the mean relative error value, reconstructing the dispersion curve in the interval (102–300) kHz for the A_0 mode and (282–420) kHz for the S_0 mode. In the best case, the dispersion curve was reconstructed with an error of 0.7% ± 1.6% for the A_0 mode and 0.5% ± 0.6% for the S_0 mode. The relative uncertainty is computed based on the phase velocities of 1999 m/s for the A_0 mode and 5380 m/s for the S_0 mode at the 300-kHz frequency.

The results obtained show a reliable estimation of the phase velocity even in highly dispersive ranges, such as the A_0 mode. It achieves mean relative errors below 1% (e.g., 0.9% in simulation and 1.7% in experimental validation). For the nearly nondispersive S_0 mode, the method also demonstrates high accuracy (mean relative errors as low as 0.1% in simulation and 1.9% in the experiment). Meantime, the STCFT method [8] using experimentally obtained A_0 mode signals at the 300-kHz frequency range resulted in an error of about 6% and for the S_0 mode of 2%. The estimated average relative error of the reconstructed phase velocity dispersion curves of both A_0 and S_0 modes was obtained within 1% using a clustering algorithm, but with ten measurement points [13]. The segment of the phase velocity dispersion curves of the A_0 mode is reproduced with an average relative error of 1.04% and for the S_0 mode of 0.6% applying the combined method [12], but using different sets of two measured signals for each mode.

Thus, a significant advantage of this method is its ability to reconstruct phase velocity dispersion curves of both A_0 and S_0 modes using signals obtained at only two measured points. This contrasts with traditional methods based on the integrated time and frequency analysis (TFA) [8], [9], which often require data from multiple measurement points along a scan line to build a full wavenumber-frequency map or computationally intensive transformations [24].

V. Conclusion

This study presents a tool for estimating the phase velocity dispersion of both the asymmetric A_0 and symmetric S_0 modes of Lamb waves using two signals measured at identical distances. In order to select two suitable measurement points, it is proposed to first calculate the maximum permissible distance between the two signals and then apply an algorithm to determine a suitable threshold level. Theoretical and experimental studies were performed using signal pairs of both A_0 and S_0 modes propagating in an aluminum plate at the same measured distances. The frequency range of 300 kHz was chosen, which indicates different dispersion levels of the A_0 and S_0 modes. Four signal pairs for each of the A_0 and S_0 modes, measured at the same distances, were employed in the theoretical analysis. The calculated mean relative error consistently remained below 0.5% in all cases. Six signal pairs at different Lamb wave propagation distances were used in the experimental study, and the average relative error remained below 2%.

A complete evaluation of errors and uncertainties was performed to assess the reliability of the given tool. The accuracy of the method is evident from the estimated relative error, which on average remains below or equal to 2% for both A_0 and S_0 modes on the reconstructed sections. The extended relative uncertainty was computed based on the phase velocities of 1999 m/s for the A_0 mode and 5380 m/s for the S_0 mode at the 300-kHz frequency. The quantitative analysis revealed that the mathematical model, dispersion curve reconstruction, and variations in the Lamb wave frequency significantly contribute to the overall uncertainty. The resulting mean relative error of 1.7% and 2% for the A_0 and S_0 modes, respectively, along with extended uncertainties of ±2.6% and ±3.2% at a 95% confidence level, demonstrate that the proposed method is a good tool for the evaluation of both A_0 and S_0 modes using only two signals measured at identical distances.

References

[1] X. Wang et al., "Ultrasonic guided wave imaging with deep learning: Applications in corrosion mapping," *Mech. Syst. Signal Process.*, vol. 169, Apr. 2022, Art. no. 108761, doi: 10.1016/j.ymssp.2021.108761.

[2] H. Zhang et al., "Damage location method of pipeline structure by ultrasonic guided wave based on probability fusion," *IEEE Trans. Instrum. Meas.*, vol. 73, pp. 1–14, 2024, doi: 10.1109/TIM.2024.3365164.

[3] Z. Wang, S. Zhang, Y. Li, Q. Wang, Z. Su, and D. Yue, "A cross-scanning crack damage quantitative monitoring and imaging method," *IEEE Trans. Instrum. Meas.*, vol. 71, pp. 1–10, 2022, doi: 10.1109/TIM.2022.3188031.

[4] S. Ding, C. Yang, and S. Zhang, "Acoustic-Signal-Based damage detection of wind turbine blades—A review," *Sensors*, vol. 23, no. 11, p. 4987, May 2023, doi: 10.3390/s23114987.

[5] B. Zima, K. Woloszyk, and Y. Garbatov, "Corrosion degradation monitoring of ship stiffened plates using guided wave phase velocity and constrained convex optimization method," *Ocean Eng.*, vol. 253, Jun. 2022, Art. no. 111318, doi: 10.1016/j.oceaneng.2022.111318.

[6] L. Draudvilienė and R. Raišutis, "Estimation of Lamb wave anti-symmetric mode phase velocity in various dispersion ranges using only two signals," *Symmetry*, vol. 15, no. 6, p. 1236, Jun. 2023, doi: 10.3390/sym15061236.

[7] P. D. Wilcox, "A rapid signal processing technique to remove the effect of dispersion from guided wave signals," *IEEE Trans. Ultrason., Ferroelectr, Freq. Control*, vol. 50, no. 4, pp. 419–427, Apr. 2003, doi: 10.1109/TUFFC.2003.1197965.

[8] Z. Su, L. Ye, and Y. Lu, "Guided Lamb waves for identification of damage in composite structures: A review," *J. Sound Vibrat.*, vol. 295, nos. 3–5, pp. 753–780, Aug. 2006, doi: 10.1016/j.jsv.2006.01.020.

[9] E. Sejdić, I. Djurović, and J. Jiang, "Time–frequency feature representation using energy concentration: An overview of recent advances," *Digit. Signal Process.*, vol. 19, no. 1, pp. 153–183, Jan. 2009, doi: 10.1016/j.dsp.2007.12.004.

[10] L. Zeng, X. Cao, L. Huang, and Z. Luo, "The measurement of Lamb wave phase velocity using analytic cross-correlation method," *Mech. Syst. Signal Process.*, vol. 151, Apr. 2021, Art. no. 107387, doi: 10.1016/j.ymssp.2020.107387.

[11] B. H. Crespo, C. R. P. Courtney, and B. Engineer, "Calculation of guided wave dispersion characteristics using a three-transducer measurement system," *Appl. Sci.*, vol. 8, no. 8, p. 1253, Jul. 2018, doi: 10.3390/app8081253.

[12] L. Draudviliene, O. Tumsys, L. Mazeika, and E. Zukauskas, "Estimation of the Lamb wave phase velocity dispersion curves using only two adjacent signals," *Compos. Struct.*, vol. 258, Feb. 2021, Art. no. 113174, doi: 10.1016/j.compstruct.2020.113174.

[13] X. Gao, Y. Tian, J. Jiao, J. Gao, and C. Li, "An accurate measurement method of Lamb wave phase velocity based on clustering algorithms," *Measurement*, vol. 195, May 2022, Art. no. 111178, doi: 10.1016/j.measurement.2022.111178.

[14] P. He, "Simulation of ultrasound pulse propagation in lossy media obeying a frequency power law," *IEEE Trans. Ultrason., Ferroelectr., Freq. Control*, vol. 45, no. 1, pp. 114–125, Jan. 1998, doi: 10.1109/58.646916.

[15] M. D. Gilchrist, "Attenuation of ultrasonic Rayleigh–Lamb waves by small horizontal defects in thin aluminium plates," *Int. J. Mech. Sci.*, vol. 41, nos. 4–5, pp. 581–594, Apr. 1999, doi: 10.1016/s0020-7403(98)00083-6.

[16] A. Vladišauskas, R. Šliteris, R. Raišutis, and G. Seniūnas, "Contact ultrasonic transducers for mechanical scanning systems," *Ultragarsas (Ultrasound)*, vol. 65, no. 2, pp. 30–35, Jun. 2010.

[17] Ö. Özdamar and J. Bohórquez, "Signal-to-noise ratio and frequency analysis of continuous loop averaging deconvolution (CLAD) of overlapping evoked potentials," *J. Acoust. Soc. Amer.*, vol. 119, no. 1, pp. 429–438, Jan. 2006, doi: 10.1121/1.2133682.

[18] H. K. Mohajan, "Two criteria for good measurements in researcg: Validity and reliability," *Ann. Spiru Haret Univ. Econ. Ser.*, vol. 17, no. 4, pp. 59–82, Dec. 2017, doi: 10.26458/1746.

[19] L. Draudviliene and A. Meskuotiene, "The methodology for the reliability evaluation of the signal processing methods used for the dispersion estimation of Lamb waves," *IEEE Trans. Instrum. Meas.*, vol. 71, pp. 1–7, 2022, doi: 10.1109/TIM.2021.3127625.

[20] L. Draudviliene, A. Meskuotiene, L. Mazeika, and R. Raisutis, "Assessment of quantitative and qualitative characteristics of ultrasonic guided wave phase velocity measurement technique," *J. Nondestruct. Eval.*, vol. 36, no. 2, p. 22, Jun. 2017,doi: 10.1007/s10921-017-0404-x.

[21] L. Draudviliene, A. Meskuotiene, O. Tumsys, L. Mazeika, and V. Samaitis, "Metrological performance of hybrid measurement technique applied for the Lamb waves phase velocity dispersion evaluation," *IEEE Access*, vol. 8, pp. 45985–45995, 2020, doi: 10.1109/ACCESS.2020.2974586.

[22] H. Czichos, T. Saito, and L. Smith Eds., *Handbook of Materials Measurement Methods*. Berlin, Germany: Springer, 2006, doi: 10.1007/978-3-540-30300-8.

[23] X. Gao, Y. Tian, J. Jiao, C. Li, and J. Gao, "Non-destructive measurements of thickness and elastic constants of plate structures based on Lamb waves and particle swarm optimization," *Measurement*, vol. 204, Nov. 2022, Art. no. 111981, doi: 10.1016/j.measurement.2022.111981.

[24] Z. Luo, L. Zeng, and J. Lin, "A novel time–frequency transform for broadband Lamb waves dispersion characteristics analysis," *Struct. Health Monitor.*, vol. 20, no. 6, pp. 3056–3074, Nov. 2021, doi: 10.1177/1475921720979283.